



# First-principles study of native defects in rutile $\text{TiO}_2$

Haowei Peng

*State Key Laboratory for Superlattices and Microstructures, Institute of Semiconductors, Chinese Academy of Sciences, PO Box 912, Beijing 100083, People's Republic of China*

Received 18 April 2007; received in revised form 30 September 2007; accepted 4 October 2007

Available online 9 October 2007

Communicated by R. Wu

## Abstract

Native point defects in the rutile  $\text{TiO}_2$  are studied via first-principles pseudopotential calculations. Except for the two antisite defects, all the native point defects have low formation energies. Under the Ti-rich growth condition, high concentrations of titanium interstitials and oxygen vacancies would form spontaneously in *p*-type samples; whereas high concentrations of titanium vacancies would form spontaneously in *n*-type samples regardless of the oxygen partial pressure.

© 2007 Elsevier B.V. All rights reserved.

**Keywords:** Defects; Rutile;  $\text{TiO}_2$ ; First-principles

## 1. Introduction

Titanium dioxide is a very important wide band-gap semiconductor applied in various areas including photocatalysis, photovoltaic cells, electronic devices, and sensors.  $\text{TiO}_2$  has three polymorphs: rutile, anatase, and brookite, among which the rutile phase is most stable. The rutile  $\text{TiO}_2$  has very high dielectric constants (86–170) [1], which makes it a candidate for replacing  $\text{SiO}_2$  as the gate material of the future [2]. Many studies, both theoretical and experimental, have been done on the rutile  $\text{TiO}_2$ , especially the surfaces [1]. There are also a few studies [3,4] on native point defects in the bulk rutile  $\text{TiO}_2$ . However, since the naturally occurring rutile is usually reduced and *n*-type, these works focus on titanium interstitial and oxygen vacancy. The electronic structure of the two defects are calculated, and in Ref. [4], the authors also calculated the formation energies of the two donor defects, yet, without charge states considered. There are total six kinds of native point defects in the rutile  $\text{TiO}_2$ : titanium interstitial ( $\text{Ti}_i$ ), titanium vacancy ( $\text{V}_{\text{Ti}}$ ), oxygen interstitial ( $\text{O}_i$ ), oxygen vacancy ( $\text{V}_{\text{O}}$ ), and two anti-site defects,  $\text{Ti}_{\text{O}}$  and  $\text{O}_{\text{Ti}}$ . With some new physics discovered, like high Curie temperature ferromagnetism in Co-doped  $\text{TiO}_2$  (both anatase and rutile) [5], it becomes necessary

to take a wider perspective on the native point defects in  $\text{TiO}_2$ . In this Letter, we calculate the formation energies, defect transition energy levels and structure properties for all the native point defect in the rutile  $\text{TiO}_2$ . Sutassana Na-Phattalung et al. compute the counterparts in the anatase  $\text{TiO}_2$  [6], and their results are compared in the discussion section.

The rest of the Letter is organized as follows. Section 2 describes our calculation method. Section 3 presents the calculated formation energies and defect structural properties. Section 4 discusses the effects of growth conditions on the formation of defects. Finally, Section 5 gives a brief summary of the Letter.

## 2. Method of calculations

The density functional calculations are performed within the local density approximation (LDA), as implemented in the Vienna ab initio simulation package (VASP) [7]. The projector augmented wave method (PAW) [8] is used to describe the ionic potentials, and the cutoff energy of the plane-wave basis set is 400 eV. For the *k*-point integration, we use a  $4 \times 4 \times 6$  Monkhorst–Pack *k* point mesh [9] for the primitive cell.

Fig. 1 shows the primitive cell of rutile  $\text{TiO}_2$ , and the calculated structural parameters are listed in Table 1, compared with the experimental values [10]. The obtained energy band gap is

E-mail address: [mypengcn@semi.ac.cn](mailto:mypengcn@semi.ac.cn).

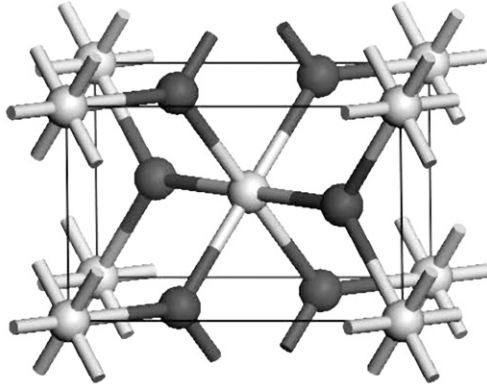


Fig. 1. The primitive cell of the rutile  $\text{TiO}_2$ . The gray atoms are titanium, and the darker ones are oxygen. The relative ionic positions are  $(0, 0, 0)$  and  $(0.5, 0.5, 0.5)$  for Ti atoms, and  $(\pm u, \pm u, 0)$ , and  $(0.5 \pm u, 0.5 \mp u, 0.5)$  for O atoms.

Table 1

Calculated structural parameters, bulk modulus, and energy gap ( $E_{\text{gap}}$ ) of rutile  $\text{TiO}_2$ , compared with the experimental results

	This work	Experimental
$a$ (Å)	4.568	4.587
$c$ (Å)	2.926	2.954
$c/a$	0.641	0.644
$u$	0.305	0.303
$B$ (GPa)	216	251
$E_{\text{gap}}$ (eV)	1.68	3.0

only 1.68 eV, which is much smaller than the experimental [10] value, 3.0 eV, due to the well-known LDA gap error.

To obtain properties of the native point defect, we use a supercell approach [11]. In this study, we model the defect system by putting the defect at the center of a  $2 \times 2 \times 3$  (72 atoms) supercell. All the internal structural parameters of the supercell are optimized until the Hellmann–Feynman force is less than 0.05 eV/Å. To calculate the charged defects, a jellium background is used to neutralize the supercell. Like in Ref. [11], we define the defect formation energy as:

$$\Delta H(\alpha, q) = \Delta E(\alpha, q) + n_{\text{Ti}}\mu_{\text{Ti}} + n_{\text{O}}\mu_{\text{O}} + q\varepsilon_F, \quad (1)$$

where  $\Delta E(\alpha, q) = E(\alpha, q) - E(0) + n_{\text{Ti}}\mu_{\text{Ti}}^0 + n_{\text{O}}\mu_{\text{O}}^0 + q\varepsilon_{\text{VBM}}$ .  $\alpha$  denotes the defect, and  $q$  is its charge state.  $n_{\text{Ti}}$ ,  $n_{\text{O}}$  denote the numbers of Ti atoms or O atoms transferred from the supercell to their corresponding reservoirs with chemical potential  $\mu_{\text{Ti}}^0$  and  $\mu_{\text{O}}^0$  respectively.  $\mu_{\text{Ti}}$  and  $\mu_{\text{O}}$  are the atomic chemical potentials of Ti atom and O atom referenced to  $\mu_{\text{Ti}}^0$  and  $\mu_{\text{O}}^0$  respectively.  $\varepsilon_F$  is the Fermi energy referenced to the valence band maximum (VBM) of rutile  $\text{TiO}_2$ .  $E(0)$  is the total energy of the  $2 \times 2 \times 3$  supercell without any defect. The defect transition energy level  $\varepsilon_{\alpha}(q/q')$  is the Fermi energy  $\varepsilon_F$  in Eq. (1) at which  $\Delta H(\alpha, q) = \Delta H(\alpha, q')$ , i.e.,

$$\varepsilon_{\alpha}(q/q') = [\Delta E(\alpha, q) - \Delta E(\alpha, q')]/(q' - q). \quad (2)$$

On the chemical potentials some limitations must be imposed to avoid forming the natural phases of the constituents (hcp Ti and  $\text{O}_2$ ), or some secondary products, for example,  $\text{Ti}_2\text{O}_3$  [6].

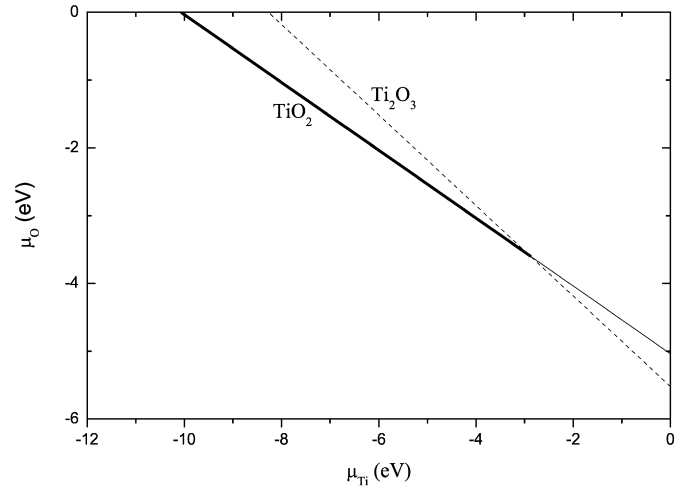


Fig. 2. The allowed values of the atomic chemical potentials  $\mu_{\text{Ti}}$  and  $\mu_{\text{O}}$ , illustrated with a bold line. Equilibrium growth of  $\text{TiO}_2$  takes place when  $\mu_{\text{Ti}}$  and  $\mu_{\text{O}}$  lying on the solid line, while equilibrium growth of  $\text{Ti}_2\text{O}_3$  happened when  $\mu_{\text{Ti}}$  and  $\mu_{\text{O}}$  lying on the dashed line.

So, the following relations must hold:

$$\mu_{\text{Ti}} \leq 0, \quad \mu_{\text{O}} \leq 0;$$

$$\mu_{\text{Ti}} + 2\mu_{\text{O}} = \mu_{\text{TiO}_2};$$

$$2\mu_{\text{Ti}} + 3\mu_{\text{O}} \leq \mu_{\text{Ti}_2\text{O}_3}. \quad (3)$$

Fig. 2 plots the available chemical potentials under equilibrium growth condition for the rutile  $\text{TiO}_2$  in the two dimensional  $(\mu_{\text{Ti}}, \mu_{\text{O}})$  plane, as defined by Eq. (3). The lines corresponding to the growth of  $\text{TiO}_2$  and  $\text{Ti}_2\text{O}_3$  intersect at  $\mu_{\text{Ti}} = -2.88$  eV. The formation of  $\text{Ti}_2\text{O}_3$  will be faster than that of  $\text{TiO}_2$ , if  $\mu_{\text{Ti}} > -2.88$  eV. So, the allowed values of  $\mu_{\text{Ti}}$  are located in the range  $[-10.07, -2.88]$ , and then  $\mu_{\text{O}}$  is determined by  $\mu_{\text{Ti}} + 2\mu_{\text{O}} = -10.07$  eV. In Fig. 2, the allowed values for  $\mu_{\text{Ti}}$  and  $\mu_{\text{O}}$  are described with a bold line.

All calculations for the supercells are done with planewave cutoff 400 eV and a  $2 \times 2 \times 2$  Monkhorst–Pack special  $k$ -point mesh. Convergence is carefully checked, with respect to both the energy cutoff and  $k$  points, taking the system with defect  $\text{Ti}_i^{4+}$  for example: when the cutoff is increased by 100 eV, the total energies of the doped supercell and the perfect one increase by 1.00 eV and 1.04 eV, respectively, both about 0.01 eV/atom; when the  $k$ -point grid is  $4 \times 4 \times 4$  (eight times the density of the one used), the total energies change 0.02 eV for both the doped and perfect supercell. So, for the formation energies (Eq. (1)), the error relating to the convergence is of the order of magnitude of 0.05 eV.

Because of the limited computational resources, we choose a system only containing 72 atoms. So the finite size errors should be considered, which result from the interaction between the defect and its periodic images. However, due to the high dielectric constant (170) [1], the correction terms is small, so we just let them alone. For example, the formation energy of the  $\text{V}_{\text{Ti}}$  calculated using a  $3 \times 3 \times 4$  (216 atoms) supercell is only about 0.35 eV larger than that calculated using the smaller su-

Table 2

Calculated formation energies ( $\Delta H$ ) of all the possible native point defects in the rutile  $\text{TiO}_2$  in different charge states under the Ti- and O-rich growth condition respectively. The Fermi level  $\varepsilon_F = \varepsilon_{\text{VBM}}$

Defect	Charge	$\Delta H$ (eV) (Ti-rich)	$\Delta H$ (eV) (O-rich)
$\text{Ti}_i$	+4	-7.20	0.01
$\text{V}_{\text{Ti}}$	-4	10.35	3.16
$\text{O}_i$	0	5.89	2.29
	-1	7.86	4.26
	-2	8.41	4.81
$\text{V}_\text{O}$	+2	-2.08	1.51
$\text{Ti}_\text{O}$	+4	-0.34	10.44
	+5	-1.21	9.58
	+6	-1.40	9.39
$\text{O}_{\text{Ti}}$	-1	16.45	5.66
	-2	16.80	6.01
	-4	18.62	7.83

percell. In summary, we estimate that the error in the calculated formation energies is about 0.4 eV.

### 3. Results

In the rutile structure, the oxygen atoms form octahedra, but only half of the octahedral sites are occupied by the titanium atoms. So, we choose an unoccupied octahedral site as the initial position for interstitial defect, which is located at the center of the (010) or (100) faces.

According to the formalism mentioned in last section, we compute the formation energies for all the defects in different charge states, at the limits of Ti-rich and O-rich conditions as shown in Fig. 2, under the  $p$ -type growth condition (the Fermi level is located at the VBM). The results are tabulated in Table 2. From the table we know that the anti-site defects have much higher formation energies than the other four defects due to the large size and chemical mismatch between Ti and O ions. The formation energy of  $\text{Ti}_\text{O}^{6+}$  is even larger than the sum of those of  $\text{Ti}_i^{4+}$  and  $\text{V}_\text{O}^{2+}$ , resulting in spontaneous disintegration. It is similar in the case of  $\text{O}_{\text{Ti}}$ , so we will not consider these two kinds of defects in the following discussion.

In Fig. 3, we plot the formation energies under both Ti-rich ( $\mu_{\text{Ti}} = -2.88$  eV, not zero) and O-rich growth conditions, as a function of the Fermi level, for the selected four defects. The slope of the line gives the charge state of the corresponding defect, and the Fermi level at the turning point gives the defect transition energy level defined in Eq. (2).

We also calculate the distances between the four defects and their nearest, second nearest neighbor titanium and oxygen atoms, respectively, which are tabulated in Table 3. For defect  $\text{V}_\text{O}$ , it is a little complicated. Because the octahedron in the rutile structure is slightly distorted, the eleven nearest oxygen neighbors of a oxygen atom break into three groups: one first nearest, eight second nearest, and two third nearest oxygen neighbors. In the table, we list all the three distances between the vacancy and its oxygen neighbors.

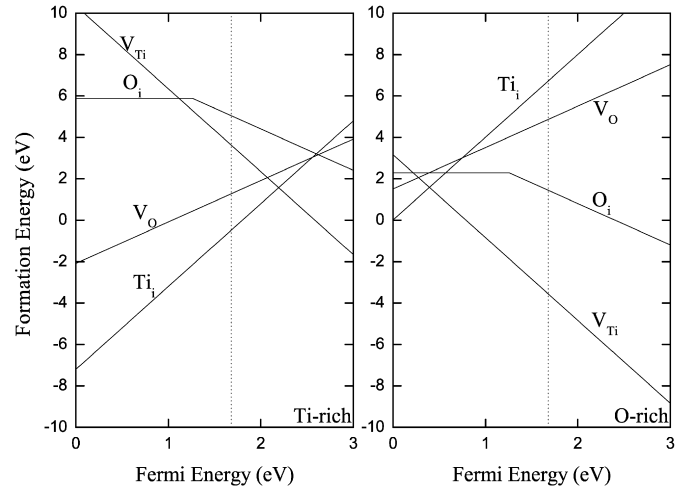


Fig. 3. Defect formation energies as a function of the Fermi level, at the Ti-rich limit (left panel) and O-rich limit (right panel), respectively. The vertical dashed line is the CBM from the first principle calculations.

Table 3

The distances between the defect and its several nearest neighbor atoms in angstroms.  $d_i(\text{X})$  stand for the distance to the  $i$ th nearest neighbor X atom, and “ideal” means the distance between the defect site and the destination site in the perfect crystal

Defect	Charge	$d_1(\text{Ti})$	$d_2(\text{Ti})$	$d_1(\text{O})$	$d_2(\text{O})$	$d_3(\text{O})$
$\text{Ti}_i$	ideal	2.284	2.712	1.651	2.206	
	+4	2.664	2.904	1.865	1.972	
$\text{V}_{\text{Ti}}$	ideal	2.926	3.546	1.937	1.961	
	-4	2.835	3.461	2.121	2.007	
$\text{O}_i$	ideal	2.284	2.712	1.651	2.206	
	0	2.044	2.876	1.776	2.430	
	-1	2.045	2.873	1.785	2.432	
$\text{V}_\text{O}$	-2	1.936	2.688	2.295	2.422	
	ideal	1.937	1.961	2.539	2.756	2.926
	+2	2.220	2.223	2.454	2.675/2.703	2.852

### 4. Discussion

#### 4.1. Titanium interstitial ( $\text{Ti}_i$ )

The titanium interstitial lies in an octahedral site similar to a lattice Ti site, but the equatorial Ti–O bond length is much longer than the apical one. After relaxation, the closest oxygen atoms, as well as the near titanium atoms are pushed away, and the equatorial oxygen atoms are pulled towards the  $\text{Ti}_i$ . As shown in Table 3, when the defect is charged +4 e, the apical and equatorial bond-lengths of the defect centered octahedron is very close to that of the lattice titanium centered octahedron.

As shown in Fig. 3,  $\text{Ti}_i$  does not introduce a defect level in the band gap, so it is not a carrier trap. Under the Ti-rich growth condition, the formation energy of  $\text{Ti}_i$  remains negative until  $E_F > 1.8$  eV. That is to say, the spontaneous formation of high concentrations of the defect as a quadruple donor makes  $\text{TiO}_2$  difficult to grow under such conditions ( $E_F < 1.8$  eV, Ti-rich), similar to the case [6] in anatase  $\text{TiO}_2$ . Under the O-rich growth condition, when the Fermi level is close to the VBM, the formation of the  $\text{Ti}_i$  is preferred.

#### 4.2. Oxygen vacancy ( $V_O$ )

Oxygen vacancy is modeled via removing an oxygen atom from the supercell in this calculation. For  $V_O$ , its three nearest neighbor titanium atoms move outward about 0.3 Å, and the nearest oxygen atoms move towards the vacancy about 0.1 Å.

$V_O$  is also not a carrier trap, and +2 is its only stable charge state. Similar to the case in the anatase [6],  $V_O$  is not a dominant native defect under equilibrium growth conditions. Under the Ti-rich growth condition, except when the  $E_F$  is near the experimental CBM, the formation of  $Ti_i$  is much easier from the view of energetics. However, oxygen vacancy is a very important native point defect in reduced rutile  $TiO_{2-x}$  experimentally. It can be introduced by special processes such as heating the specimen in oxygen at reduced pressure [12] or vacuum annealing. On the other hand, although due to the larger formation energies,  $V_O$ 's may convert to  $Ti_i$ 's via reaction:  $mTiO_2 + 2nV_O \rightarrow (m - n)TiO_2 + nTi_i$ , six Ti–O bonds have to be broken to free a titanium atom, while only three to free an oxygen atom. Besides, the number of possible sites for  $V_O$  is twice of that for  $Ti_i$ . So, from the view of kinetics, the formation of the  $V_O$  is more favored than that of the  $Ti_i$ , given the same formation energy. Especially, at the pinned Fermi level (about 2.2 eV and 0.5 eV at the Ti- and O-rich condition, respectively, as showed in Fig. 3), the formation energies of the  $V_O$  and  $Ti_i$  are very close. So, high concentrations of  $V_O$ 's also may form under the equilibrium growth conditions.

#### 4.3. Titanium vacancy ( $V_{Ti}$ )

When a titanium vacancy forms, the nearest Ti atoms move to the vacancy about 0.1 Å, and the nearest oxygen atoms relax outward about 0.2 Å. Fig. 3 illustrates that  $V_{Ti}$  is not a carrier trap, and its charge state is –4. Under the O-rich growth condition, as long as  $E_F > 0.8$  eV, it has a negative formation energy, and it is very easy to form. From the right panel of the figure, we conclude that the undoped rutile  $TiO_2$  tends to be *p*-type at the O-rich limit, since the Fermi level will be pinned close to the VBM. Because, if the Fermi level is higher, the acceptors  $V_{Ti}^{4-}$  will form and compensate the electrons. Similarly, under Ti-rich growth conditions, the undoped rutile  $TiO_2$  tends to be *n*-type. Meanwhile, under the Ti-rich growth condition, when  $E_F$  is above 2.6 eV, the formation energy is also negative. Due to its low formation energies, titanium vacancy is the leading acceptor point defect.

#### 4.4. Oxygen interstitial ( $O_i$ )

In Ref. [6], the isolated interstitial oxygen in the anatase  $TiO_2$  is reported to be unstable, and it forms a substitutionary  $O_2$  molecule via binding with a lattice oxygen. But in the rutile  $TiO_2$ , the case is different. As an oxygen atom occupies the center of the octahedron, its nearest titanium ions are attracted, while the oxygen ions are pushed away. As tabulated in Table 3

the atomic position of the oxygen interstitial is very sensitive to the charge state. This suggests that  $O_i$  is a negative-*U* system. Actually, Fig. 3 shows that for  $O_i$  the  $q = -1$  charged state is unstable with respect to dissociating into the  $q = -2$  and  $q = 0$  charge states, and the defect transition energy level  $\epsilon(2 - /0) = 1.26$  eV. Under the Ti-rich growth condition, the oxygen interstitial has a high formation energy, while under the O-rich growth condition, large concentrations of it can form if  $E_F$  is above around 2.5 eV.

### 5. Conclusions

In conclusion, our calculations provide detailed information for native defects in the rutile  $TiO_2$ .  $Ti_i$ ,  $V_{Ti}$ ,  $O_i$ ,  $V_O$  all have low formation energies.  $Ti_i$ ,  $V_{Ti}$ ,  $V_O$  do not introduce defect levels inside the DFT band gap.  $Ti_i$  is a quadruple donor defects, and  $V_O$  can co-exist with it from the point of view of kinetics. Both of their formation energies are enhanced under the Ti-rich growth condition.  $V_{Ti}$  is the leading quadruple acceptor, with very low formation energy under the O-rich growth condition.  $O_i$  is a negative *U* system, and its formation benefits from the O-rich growth condition. Under O-rich growth conditions, the undoped rutile  $TiO_2$  tends to be *p*-type, and under Ti-rich growth conditions, *n*-type is favored. The two antisite defects,  $Ti_O$  and  $O_{Ti}$ , have high formation energies and are unstable. Finally, there are errors resulting from the finite size, basis set, and *k*-point sampling used in the present calculation, as well as the underestimated LDA gap, but the main conclusions would remain unchanged.

### Acknowledgements

This work was supported by the National Natural Science Foundation of China under Grant Nos. 60325416, 60521001, and 90301007.

### References

- [1] U. Diebold, Surface Sci. Rep. 48 (2003) 53, and references therein.
- [2] S.A. Campbell, H.-S. Kim, D.C. Gilmer, B. He, T. Ma, W.L. Gladfelter, IBM J. Res. Dev. 43 (1999) 383.
- [3] N. Yu, J. Woods Haley, Phys. Rev. B 51 (1995) 4768.
- [4] E. Cho, S. Han, H.-S. Ahn, K.-R. Lee, S.K. Kim, C.S. Hwang, Phys. Rev. B 73 (2006) 193202.
- [5] T. Fukumura, H. Toyosaki, Y. Yamada, Semicond. Sci. Technol. 20 (2005) S103.
- [6] S. Na-Phattalung, M.F. Smith, K. Kim, M.-H. Du, S.-H. Wei, S.B. Zhang, S. Limpijumnong, Phys. Rev. B 73 (2006) 125205.
- [7] G. Kresse, J. Furthmüller, Comput. Mater. Sci. 6 (1996) 15.
- [8] G. Kresse, J. Joubert, Phys. Rev. B 59 (1999) 1758.
- [9] H.J. Monkhorst, J.D. Pack, Phys. Rev. B 13 (1976) 5188.
- [10] J.K. Burdet, T. Hughbanks, G.J. Miller Jr., J.V. Smith, J. Am. Chem. Soc. 109 (1987) 3639.
- [11] S.-H. Wei, S.B. Zhang, Phys. Rev. B 66 (2002) 155211.
- [12] F.A. Grant, Rev. Mod. Phys. 31 (1959) 646.